Purification of polyhydroxybutyrate synthase from its native organism, *Ralstonia eutropha*: implications in the initiation and elongation of polymer formation in vivo

Mimi Cho[1], **Christopher J. Brigham**[2], **Anthony J. Sinskey**[2,3,4], and **JoAnne Stubbe**[1,2,*]

[1]Department of Chemistry, Massachusetts Institute of Technology, 77 Massachusetts Avenue, Cambridge, MA, 02139, USA

[2]Department of Biology, Massachusetts Institute of Technology, 77 Massachusetts Avenue, Cambridge, MA, 02139, USA

[3]Division of Health Sciences Technology, Massachusetts Institute of Technology, 77 Massachusetts Avenue, Cambridge, MA, 02139, USA

[4]Engineering Systems Division, Massachusetts Institute of Technology, 77 Massachusetts Avenue, Cambridge, MA, 02139, USA

Abstract

Class I polyhydroxybutyrate (PHB) synthase (PhaC) from *Ralstonia eutropha* catalyzes the formation of PHB from (*R*)-3-hydroxybutyryl-CoA, ultimately resulting in the formation of insoluble granules. Previous mechanistic studies of *R. eutropha* PhaC, purified from *Escherichia coli* (PhaC$_{Ec}$), demonstrated that the polymer elongation rate is much faster than the initiation rate. In an effort to identify a factor(s) from the native organism that might prime the synthase and increase the rate of polymer initiation, an *N*-terminally Strep2-tagged *phaC* (Strep2-PhaC$_{Re}$) was constructed and integrated into the *R. eutropha* genome in place of the wt-*phaC*. Strep2-PhaC$_{Re}$ was expressed and purified by affinity chromatography from *R. eutropha* grown in nutrient-rich TSB medium for 4 h (peak production PHB, 15% cdw) and 24 h (PHB, 2% cdw). Analysis of the purified PhaC by size exclusion chromatography, SDS-PAGE and gel permeation chromatography revealed that it unexpectedly co-purified with the phasin protein, PhaP1, and with soluble PHB (M$_w$ 350 kDa) in a "high molecular weight" (HMW) complex and in monomeric/dimeric (M/D) forms with no associated PhaP1 or PHB. Assays to monitor PHB formation in the HMW complex showed no lag phase in CoA release, in contrast to M/D forms of PhaC$_{Re}$ (and PhaC$_{Ec}$), suggesting that PhaC in the HMW fraction has been isolated in a PHB-primed form. The presence of primed and non-primed PhaC suggests that the elongation rate for PHB formation is also faster than the initiation rate in vivo. A modified micelle model for granule genesis is proposed to accommodate the reported observations.

*Corresponding author: stubbe@mit.edu, Phone: (617) 253-1814, Fax: (617) 324-0505.

Keywords

Ralstonia eutropha; native and primed PHB synthase; Strep2 tag; soluble granules

Polyhydroxybutyrate (PHB) synthase, PhaC, catalyzes the polymerization of (*R*)-3-hydroxybutyryl-coenzyme A (HBCoA) to PHB. These polyoxoesters are produced and packaged into insoluble, inclusions or granules by a variety of bacteria as carbon storage compounds, when the bacteria are faced with nutrient-limited growth conditions in the presence of an abundant carbon source (1–5). When the environment is more conducive to replication, the biopolymers are degraded and the liberated energy and monomers are used for cell growth and division. PHBs and copolymers of PHB and polyhydroxyvalerate (PHV) are of general interest because they are biodegradable thermoplastics. Understanding the polymerization process resulting in PHB of high molecular weight and low polydispersity and the genesis of PHB granules is important to optimizing the metabolic engineering of organisms to produce PHB/PHV and other polyoxoesters in an economically competitive fashion with environmentally unfriendly, petroleum-based plastics (6, 7). Thus far, synthases have primarily been isolated from recombinant expression in *Escherichia coli*, which does not have the biosynthetic machinery for PHB production (8–13). This paper reports the first isolation of a synthase from its native organism, *Ralstonia eutropha* and the unexpected observation that it co-purifies with PHB and the phasin protein PhaP1 in a soluble form. The former observation suggests isolation of PHB-primed PhaC and the latter observation suggests isolation of soluble granule precursors, providing insight into insoluble granule formation.

R. eutropha, which possesses a class I synthase, is the best characterized PHB-producing organism (1, 4, 14, 15). Biochemical studies using *R. eutropha* synthase expressed and purified from *E. coli* (PhaC$_{Ec}$) have shown that the polymerization process involves covalent catalysis requiring an active site cysteine (16). Kinetic studies monitoring CoA release as an indicator of polymer formation reveal a lag phase that is dependent on the concentration of the enzyme (8, 14, 17) and that the lag phase can be reduced and the activity increased by artificially priming PhaC$_{Ec}$ with a trimer or saturated trimer of HBCoA ((HB)$_3$CoA or sTCoA, Figure 1) (14, 16). The synthase has been shown to exist in monomeric and dimeric forms and priming of the synthase with sTCoA shifts the equilibrium to the dimeric form, suggesting that the synthase is active as a dimer (16). Kinetic studies further reveal that the elongation rate is much faster than the initiation rate; that is, a small amount of PhaC$_{Ec}$ catalyzes formation of a large PHB polymer, while most of the PhaC remains unreacted (8, 18). If the kinetics of polymerization are similar in vivo, then it is difficult to understand how the cell controls the generation of granules in which all of the proteins involved in PHB homeostasis are located on their exterior with amorphous PHB on their interior (19–22). Thus we proposed that a factor(s) might be present in *R. eutropha* that primes the synthase, allowing control of the polymer initiation rate relative to its elongation rate which in turn, would facilitate controlled granule formation.

A number of protein factors have been identified by their association with purified PHB granules or by bioinformatics, but no candidates for a protein initiation factor(s) have been reported (3, 4). The phasin protein PhaP1 is of particular interest as it is the most abundant granule associated protein (21). Its expression is induced by PHB (23) and its expression levels increase concomitant with PHB production (24, 25). In contrast, PhaC is constitutively expressed (25, 26) at substantially lower levels relative to PhaP1. At maximum PHB production in rich, tryptic soy broth (TSB) medium or in nitrogen limited medium (PHB$_{High}$), the granules range in size from 0.2 to 0.5 μm in diameter and each granule has one to two molecules of PhaP1 per PHB chain and 50 to 100 PhaC molecules

per PHB chain requiring many chain termination and re-initiation events during granule formation (25). PhaP1 controls the amount (23, 24), the size, and the number of the granules (21) and likely prevents PHB crystallization (27). While other putative phasin proteins (PhaP2-PhaP5, PhaP1 homologs) have been identified, their expression levels are low compared to PhaP1 (28–30). Other proteins associated with granules include PhaR, a transcription factor that negatively regulates PhaP1 expression (31, 32), and the PhaZ proteins, which are intracellular depolymerases (33–35). These protein factors are associated with the surface of the PHB granules based on immunogold labeling studies (20, 21, 31), but only PhaP1 contributes substantially (14–28%) to the granule surface coverage (25, 36).

Our initial objective in the studies described herein was to identify an initiation factor via isolation of the synthase from its native organism. For this purpose, a strain of *R. eutropha* was constructed in which an *N*-terminal Strep2-tagged-*phaC* gene was integrated in place of the wt-*phaC* gene in the *R. eutropha* genome in order to express an affinity-tagged synthase under its endogenous promoter. We chose rich, TSB medium for growth conditions, under which PHB is transiently produced (Figure S1). Under these conditions, the amount of PHB in the cells increases to a maximum of ~15% of the cell dry weight (cdw) at 4 h, and then declines to 2% over 24 h due to degradation of the PHB chains (25). To facilitate PhaC purification, we initially chose to isolate the synthase after 24 h cultivation to minimize the amount of PHB in the cells and thus, the amount of PhaC associated with insoluble granules precluding its isolation (8, 25, 37). The affinity tag allowed rapid purification of PhaC which was analyzed by SDS-PAGE and by size exclusion chromatography (SEC). Surprisingly by SEC, PhaC eluted in a soluble high molecular weight (HMW) fraction containing PHB and PhaP1 as well as in a dimeric/monomeric form without PHB or PhaP1. Furthermore, assays of the PhaC in the HMW fraction revealed no lag phase in CoA release. Thus although no candidate protein for an initiation factor was identified by SDS-PAGE, our studies suggested that a PHB-primed synthase was isolated for the first time (16). We then focused on purification of PhaC from cells cultivated in TSB medium for 4 h (Figure S1) when PHB production was maximized. Our prior transmission electron microscopy (TEM) studies showed that small, "initiating" granules as well as 0.2 μm diameter granules are present at this time point (25) and recent cryoelectron tomography studies suggest nascent granules are continually generated during PHB production (38). Therefore, we predicted that this growth condition might allow isolation of soluble granule precursors, providing insight into the mechanism of granule formation. Again, a soluble HMW fraction that includes PhaC, PhaP1, and high molecular weight PHB was isolated by SEC. These results suggest that we have isolated a primed synthase from a native organism and that PHB functions in this capacity. They also suggest that the elongation rate for PHB polymerization is much faster than the initiation rate in vivo. Finally the isolation of a soluble PhaC/PhaP1/PHB complex precludes a membrane budding model for the mechanism of granule genesis and suggests an alternative micelle model.

Experimental Procedures (Materials and Methods)

Materials

All strains and plasmids used in this study are listed in Table 1. All chemicals were purchased in highest purity available from Sigma-Aldrich (St. Louis, MO) unless otherwise specified. Oligonucleotide primers were purchased from Integrated DNA Technologies (Coralville, IA). *Taq* DNA polymerase was purchased from Qiagen (Valencia, CA) and other DNA modification enzymes were purchased from New England Biolabs (Beverly, MA). *(R)*-3-hydroxybutyryl-CoA (HBCoA) was synthesized as previously described (15).

Protein quantitation and sequencing

PhaC concentration was based on A_{280} ($\varepsilon = 162{,}000$ M^{-1} cm^{-1}) (15). For heterogeneous mixtures of protein, PhaC and PhaP1 concentrations were determined by quantitative Western blotting, as detailed below. Total protein concentrations in heterogeneous mixtures were determined by Bradford assay using BSA as a standard (39). Protein *N*-terminal sequencing was performed by Tufts University School of Medicine Core Facility.

Enzyme assays

Assays were carried out as previously described (14) with the concentration of PhaC at 30–60 nM. The average specific activity from three assays performed at three different enzyme concentrations is reported where one unit of activity is defined as 1 μmol CoA released per min (14).

Construction of a N-terminally tagged strep2-(G$_4$S)$_3$-phaC (strep2-phaC) for expression in E. coli

For construction of a *strep2-phaC*, *phaC* from *R. eutropha* strain H16 was amplified by PCR using the forward primer phaCSTREPFW and the reverse primer phaCSTREPRV (Table 2) to introduce a *Bam*HI restriction site followed by the coding sequence for a (G$_4$S)$_3$ linker at the 5′ end of *phaC* and a *Hin*dIII restriction site at the 3′ end. The amplified gene was cut with the appropriate restriction enzymes and ligated into pET51b (Novagen), containing the gene sequence for an *N*-terminal Strep2-(G$_4$S)$_3$-tag, to produce pCJB16. The portion of pCJB16 containing the tagged *phaC* was sequenced by the MIT Biopolymers Laboratory.

Integration of the strep2-phaC into the R. eutropha chromosome in place of wt-phaC (23, 24)

The plasmid pJV7 (40), a derivative of pJQ200mp18Km containing kan resistance (*kan^R*) and sucrose sensitivity (*sacB*) markers for homologous recombination (41), was utilized for integration of the *strep2-phaC* into the *R. eutropha* chromosome. In order to generate pJV7, the deletion allele of *phaC$_{Re}$* (Δ*phaC*) was inserted into the *Bam*HI site in the multiple cloning region of pJQ200mp18Km. The Δ*phaC* allele consists of the 0.41 kb sequence located immediately upstream of the *phaC$_{Re}$* open reading frame (ORF) ligated adjacent to the 0.45 kb sequence located immediately downstream of the *phaC$_{Re}$* ORF via a *Swa*I restriction site. For insertion of *strep2-phaC* into pJV7, the gene was first excised from pCJB16 by digestion with *Hin*dIII and *Xba*I. The gene was blunt ended using the Klenow fragment (New England Biolabs) and then ligated into the *Swa*I site of pJV7 to create pCJB4 (Table 1).

The resulting plasmid was introduced into *R. eutropha* Re1034 (Δ*phaC*) (23) by conjugation with *E. coli* S17-1/pCJB4. Transconjugants of *R. eutropha*, in which pCJB4 was inserted into the genome in the first recombination event, were selected by plating on tryptic soy agar supplemented with 0.2% fructose, 10 μg/mL gentamicin (gent) to select for *R. eutropha*, and 300 μg/mL kanamycin (kan) to select for the recombination event. These transconjugants were then grown in TSB medium supplemented with 10 μg/mL gent for 24 h at 30 °C and spread on tryptic soy agar with 0.2% fructose, 10 μg/mL gent, and 5% sucrose to select for the second recombination event in which the plasmid pCJB4 is excised from the genome to produce the desired mutant strain. All sucrose resistant colonies were tested for kan sensitivity to ensure the loss of the pCJB4 insert. They were also tested for PHB production, indicating the presence of a functional Strep2-PhaC$_{Re}$. PCR was used to confirm the presence of a *strep2-phaC* gene replacement. The resulting strain, Re2018, was used for purification of Strep2-PhaC$_{Re}$.

Construction of C319A-strep2-phaC

Primers *phaC*C319A and *phaC*C319A-GC (Table 2) were used in conjunction with the QuikChange® II Site-Directed Mutagenesis Kit (Stratagene, La Jolla, CA) to mutagenize the codon for the active site cysteine (TGC) to an alanine (GCG) and create pCJB16-C319A (Table 1). The resulting *C319A strep2-phaC* was excised from pCJB16-C319A and inserted into the *R. eutropha* chromosome as described above.

Growth of E. coli BL21(DE3)/pCJB16 and purification of Strep2-PhaC$_{Ec}$

All culture medium was supplemented with 100 μg/mL ampicillin (amp). A single colony of BL21(DE3)/pCJB16 cells from an LB plate was used to inoculate 5 mL of LB culture broth. Cells were grown overnight at 37 °C. The entire culture was used to inoculate 1 L of LB at 37 °C. Cells were grown to an $OD_{600} = 0.6$, and the expression of Strep2-PhaC$_{Ec}$ was induced by addition of 0.1 mM isopropyl-β-thiogalactoside (IPTG). Cells were then grown at 30 °C for an additional 2 h. Cells (~5 g wet weight) were pelleted by centrifugation at $3,000 \times g$ at 4 °C. The cell pellet was re-suspended in 25 mL of 100 mM Tris-HCl, pH 8.0, 0.05% Hecameg and lysed using a French pressure cell (2 passes at 12,000 psi). The resulting cell lysate was centrifuged at $100,000 \times g$ to remove cell debris. The clarified lysate (25 mL, 3.5 mg protein/mL) was loaded onto a Strep-tactin column (IBA, GmbH, Göttingen, Germany; 10 mL column volume) pre-equilibrated with buffer A (100 mM Tris-HCl, pH 8.0, 150 mM NaCl, 1 mM EDTA). The lysate and column were incubated at 4 °C for 15–20 min. The column was washed with 5×20 mL of buffer A containing 0.05% Hecameg. Strep2-PhaC$_{Ec}$ was eluted from the column with 30 mL of buffer A containing 0.05% Hecameg, 1 mM desthiobiotin, and 10% glycerol and 5 mL fractions were collected. Hecameg detergent (Sigma) was added to the buffers to improve Strep2-PhaC recoveries from the column as previously described (8). Concentrations of Hecameg were 10-fold below the critical micelle concentration. Fractions containing Strep2-PhaC as determined by SDS-PAGE and A_{280}/A_{260} were pooled and concentrated using a Vivaspin 6 concentrator (Sartorius AG, Göttingen, Germany) to 5 mg/mL and stored at −80 °C. Protein (12.5 mg/g cells) of specific activity 39 ± 11 U/mg was obtained.

Growth of Re2018 for purification of Strep2-PhaC$_{Re}$

All culture medium was supplemented with 10 μg/mL gent and all growths were at 30 °C. A single colony of *R. eutropha* Re2018 (Table 1) was used to inoculate 5 mL of TSB culture broth. The culture was grown overnight and was used to inoculate 250 mL of TSB in a 2.8-L baffled flask, which was then also grown overnight. The 250 mL culture was used to inoculate to an initial OD_{600} of 0.5, either 3 L of TSB in a 4-L BioEngineering L1523 fermentor (Wald, Switzerland) or 8 L of TSB in a 10-L New Brunswick Microferm fermentor (Edison, NJ). Cells were grown for 24 h at 400 rpm in the 4-L fermentor (Strep2-PhaC$_{Re24h}$) or 4 h at 500 rpm in the 10-L fermentor (Strep2-PhaC$_{Re4h}$). In both fermentations, aeration was maintained by sparging with air at 1 volume of air per volume of culture per min. The pH was not controlled. Cells were harvested by centrifugation at $3,000 \times g$ for 20 min at 4 °C giving cell paste of 20 g/L (24 h culture) and 4 g/L (4 h culture).

Purification of Strep2-PhaC$_{Re24h}$

The cell pellet (40 g) was re-suspended in 240 mL of 100 mM Tris-HCl, pH 8.0, 0.05% Hecameg and lysed by 2 passes in a French pressure cell at 12,000 psi. The cell debris was removed by centrifugation at $100,000 \times g$, and 10 mL of Strep-tactin resin was added to the supernatant, which was stirred at 4 °C for 30 mins. The resin was loaded into a column and was washed with 100 mL of buffer A containing 0.05% Hecameg. Strep2-PhaC$_{Re24h}$ was eluted using 30 mL of buffer A containing 0.05% Hecameg, 1 mM desthiobiotin, and 10%

glycerol and 5 mL fractions were collected. Fractions containing Strep2-PhaC as determined by SDS-PAGE and A_{280}/A_{260} were pooled and concentrated using a Vivaspin 6 concentrator to 8 mg/mL and stored at −80 °C. Protein (0.14 mg/g cells) of specific activity ranging from 30 – 90 U/mg was obtained, based on three different purifications.

Purification of Strep2-PhaC$_{Re4h}$

The purification was similar to that for Strep2-PhaC$_{Re24h}$ except that a cell pellet of 1 g was re-suspended in 5 mL of 100 mM Tris-HCl, pH 8.0, 0.05% Hecameg and 2 U/mL of DNase (New England Biolabs). Crude extract was incubated with the DNase for 30 min during cell lysis. After lysis, cell debris was removed by centrifugation at $30,000 \times g$ and 5 mL of the Strep-tactin resin was added to the supernatant. All wash and elution volumes described above were reduced by a factor of 2. Protein (0.72 mg/g cells) of specific activity ranging from 35 – 100 U/mg was obtained, based on four different purifications.

Size Exclusion Chromatography (SEC)

Purified Strep2-PhaC$_{Ec}$, Strep2-PhaC$_{Re4h}$, or Strep2-PhaC$_{Re24h}$, 500 μg, was injected onto a Bio-Sil SEC 250-5 column (M_w range = 10,000 – 300,000 Da, Bio-Rad, Hercules, CA) attached to a Waters 515/2487 HPLC system at room temperature (RT). The eluent was 50 mM KP$_i$, pH 7.6, 150 mM NaCl, and 0.05% Hecameg and the flow rate was 0.5 mL/min. Fractions, 200 μL, were collected in a 96-well plate on ice. Each fraction was monitored for A_{280} using a plate reader (BioRad Ultramark EX). Fractions corresponding to the high molecular weight (HMW), dimeric, and monomeric Strep2-PhaC species were pooled and concentrated to 1 mg/mL protein using a Vivaspin 6 concentrator. Samples were analyzed via SDS-PAGE and assayed for activity and PHB content via the crotonic acid assay (42). Retention times of the different fractions containing Strep2-PhaC were compared with retention times of molecular weight standards (Bio-Rad): bovine thyroglobulin (M_w = 660 kDa, elution time = 13.8 min), bovine γ-globulin (158 kDa, 16.1 min), chicken ovalbumin (44 kDa, 17.1 min), horse myoglobin (17 kDa, 20.9 min), and vitamin B$_{12}$ (1350 Da, 24.0 min).

Quantification of PHB in whole cells and associated with PhaC$_{Re}$

R. eutropha H16 (wt) and Re2018 (*strep2-phaC*) cells grown in TSB as described above were dried at 80 °C (10–20 mg after drying) and used to determine the levels of PHB in whole cells as described below. To determine the amount of PHB associated with purified protein samples [Strep2-PhaC$_{Ec}$ (2 mg), Strep2-PhaC$_{Re4h}$ (120 μg), Strep2-PhaC$_{Re24h}$ (1 mg), or fractions of Strep2-PhaC$_{Re}$ (30 to 500 μg) isolated by SEC-HPLC; amounts determined by Bradford assays], each sample was added to a borosilicate tube and heated overnight in vacuo at 80 °C. Samples were then dissolved in 1 mL of concentrated H_2SO_4 and PHB quantitation was performed using the crotonic acid assay (42). Samples or dilutions of samples (25 μL) were injected onto a BioRad Aminex HPX-87H organic acid column attached to an Agilent 1100 series HPLC and eluted at a flow rate of 0.6 mL/min at 50 °C with 5 mM H_2SO_4. Elution was monitored by A_{210}. The retention time for crotonic acid was 29 min. Standard curves of peak area versus PHB concentration (2–200 μg/mL) were generated using commercially available PHB (Sigma).

Quantitative Western blotting

Samples of purified Strep2-PhaC$_{Re4h}$ before SEC and the HMW fraction of Strep2-PhaC$_{Re4h}$ (20–30 ng protein) were resolved on 10% SDS-PAGE for Strep2-PhaC or 15% SDS-PAGE for PhaP1. Protein was blotted onto a PVDF membrane (Immun-Blot, BioRad) at 100 V for 80 min on ice using a Criterion wet blotting apparatus (BioRad). The blotting buffer for Strep2-PhaC sample was 25 mM Tris, 192 mM glycine, 20% (v/v) methanol, and

0.01% (w/v) SDS and for PhaP1, the blotting buffer was identical with 15% (v/v) methanol. Blots were blocked in 3% (w/v) milk in Tris-acetate-EDTA (TAE) buffer containing 0.1% (v/v) Tween 20. The primary rabbit antibodies for PhaP1 were purified by acetone powder extraction using the Re1052 (Δ*phaP1*) strain (24, 43). Blots were incubated with anti-PhaC antibody (diluted 1:5000) or anti-PhaP1 antibody (diluted 1:2500) in blocking buffer for 1 h at RT. Goat anti-rabbit antibody, conjugated with horseradish peroxidase (Thermo Scientific, Rockford, Ill.), was used as the secondary antibody (1:2000). All membranes were developed using SuperSignal® West Femto chemiluminescent detecting reagents (Thermo Scientific). Signals were detected using a BioRad ChemiDoc XRS imager and analyzed with Quantity-One® 1-D software (BioRad). The protein standard curves were generated with Strep2-PhaC$_{Ec}$ (0.5 to 10 ng) and PhaP1 (2 to 15 ng) purified from *E. coli*.

For quantitative whole cell Western blots, samples were normalized based on the OD$_{600}$ of the cells used for sample preparation. Generally, 10 μL of the cell suspension (OD$_{600}$ from 1–10, depending on whether a PhaP1 or PhaC Western blot was performed) in Laemmli buffer was loaded (44). For standard curve generation, Re1052 and Re1034 (Table 1) cell samples in Laemmli buffer were spiked with 2 to 15 ng purified PhaP1 and 0.5 to 10 ng purified Strep2-PhaC$_{Ec}$ respectively immediately prior to gel loading for blotting consistency. All blotting conditions were the same as above.

Extraction of PHB and Gel Permeation Chromatography (GPC) analysis

Soluble and insoluble fractions of the crude extract of Re2018 or Strep2-PhaC$_{Re4h}$ (3–200 mg) were lyophilized in a glass vial. PHB was extracted directly from the resulting residue by refluxing in chloroform at 70 °C for 48 h with stirring. After cooling to RT, the samples were filtered through a 4 mm syringe filter containing a 0.45 μm PTFE membrane (Whatman, Piscataway, NJ) to remove insoluble material. Sample volumes were adjusted to a final concentration of 3 mg/mL PHB as determined by the crotonic acid assay. Samples (100 μL) were injected onto $2 \times 300 \times 7.5$ mm Plgel Olexis columns (Varian, Palo Alto, CA) attached to an Agilent 1100 series HPLC fitted with refractive index detection and products were eluted at a flow rate of 1 mL/min at 30 °C with chloroform. Retention times of sample peaks were adjusted based on an internal isopropanol standard (retention time, 21.0 min) and compared with polystyrene narrow molecular weight standards (Varian) with sizes (retention time): 1.1 kDa (18.6 min), 3.1 kDa (17.9 min), 10 kDa (17.0 min), 25 kDa (16.4 min), 72 kDa (15.6 min), 210 kDa (14.9 min), 490 kDa (14.2 min), 1800 kDa (13.2 min), and 5000 kDa (12.9 min). To determine the M_p, M_n, and M_w of each sample, Agilent GPC add-on (Rev B.01.01) software was used.

Results

Construction of strep2-phaC gene and the corresponding replacement strain Re2018

In order to purify PhaC from the native organism, several gene constructs encoding different *N*-terminal affinity-tagged PhaCs with various linkers for expression in both *E. coli* and *R. eutropha* were generated. Initially, a (His)$_6$-PhaC with no linker was investigated. Expression and isolation of this construct from *E. coli* yielded homogenous protein and excellent recoveries. However, attempts to purify the same protein after integration of the gene into the *R. eutropha* genome were unsuccessful due to weak binding of the tag to the Ni^{2+} affinity resin (45). Thus, a Strep2 tag, with the amino acid sequence WSHPQFEK, was investigated (46). Ultimately, the *strep2-phaC* construct encoding a linker with the triplicate repeat of four glycines and one serine, (G$_4$S)$_3$, between the tag and PhaC was chosen for further study. Isolation of the protein expressed in *E. coli* BL21(DE3) yielded homogenous enzyme with a lag phase in CoA release (Figure 2) and a specific activity of 39 ± 11 U/mg, similar to the activity of the untagged PhaC previously reported, 40–50 U/mg (16). The

variability in the specific activity is due to difficulty in identifying the linear part of the activity curve as described in Figure S2.

Given the comparable activity of the Strep2-PhaC$_{Ec}$ and the untagged-PhaC, the gene construct was incorporated into the *R. eutropha* genome in place of the *wt-phaC* to generate strain Re2018 (23, 24). Rich TSB medium (25) was chosen for growth of Re2018 instead of nitrogen limited medium (24) for maximize PHB production, in order to minimize the amount of PhaC bound to insoluble granules which has previously defied purification by many groups (8, 37). Growth of Re2018 in TSB medium resulted in maximum production of PHB by 4 h (15%), which then dropped substantially by 24 h (Figure S1) as PHB is degraded to replace the depleted carbon source. A similar trend has been observed for wt *R. eutropha* H16 in TSB medium (25). Analysis of the amounts of PhaC in the Re2018 and wt strains using quantitative Western blots on whole cells showed 35-fold up-regulation in the mutant strain during parallel growths in shake flasks (Figure S3A). Expression of the phasin protein PhaP1 was increased 1.5 fold (Figure S3A). The up-regulation of PhaC production was not expected, is not understood, and is likely the result from insertion of the *strep2*-tag into the *phaCAB* operon. Recent studies have shown that insertions into the *phaCAB* operon can affect expression from this operon (47). The up-regulation of PhaC may fortuitously have played a role in our ability to isolate soluble granules described subsequently.

Purification of Strep2-PhaC$_{Re24h}$

Initial purification efforts focused on Strep2-PhaC from cells grown in TSB medium for 24 h (Figure S1), conditions to minimize the amount of PhaC associated with insoluble granules. Chromatography on a Strep-tactin column yielded a highly purified enzyme with a specific activity ranging from 30 – 90 U/mg (Strep2-PhaC$_{Re24h}$, Table S2), based on three different purifications. In contrast with PhaC$_{Ec}$ assayed at the same concentration, however, there was no lag phase in the release of CoA (Figure 2), unexpectedly suggesting the presence of a PHB-primed synthase (16). The broad range in specific activities measured is likely associated with variability in the extent of primed synthase within and between different purifications (Figure 2, Figure S2) (16).

Identification of proteins copurifying with Strep2-PhaC$_{Re24h}$

By affinity chromatography isolation of Strep2-PhaC$_{Re24h}$ from the host organism, we hoped to identify a factor(s) that could increase the initiation rate of the polymerization process relative to the elongation rate and consequently provide insight into the priming process in vivo. Thus, we examined the affinity purified Strep2-PhaC$_{Re24h}$ by SDS-PAGE (Figure 3A, lane 2). In addition to PhaC (64 kDa), five proteins with molecular weights of 20, 32, 45, 60, and 75 kDa were observed and subjected to *N*-terminal sequencing analysis. Each of the co-purifying proteins was identified (Table S1), but none appeared to be a reasonable candidate for a primer of the synthase (35).

The 60 and 75 kDa proteins are annotated as the β and α subunits of an acetyl/propionyl-CoA carboxylase (Accession # Q0KA97 and # Q0KA96), the first committed step of fatty acid biosynthesis (35). The α subunit of this enzyme is biotinylated, is known to co-purify with the β subunit, and therefore likely co-purified with PhaC due to affinity for the Strep-tactin resin. These same proteins were earlier reported to co-purify with Strep2-tagged [NiFe]-hydrogenases from *R. eutropha* H16 (48) using this resin. The 45 kDa protein is annotated as a hypothetical protein (Accession # Q0K3J8). A BLAST search showed that the protein is 84% identical to a sulfotransferase in *R. eutropha* JMP134 and is an unlikely candidate for PhaC priming. The 32 kDa protein is identified as a hypothetical, membrane-associated protein (Accession # Q0KFC8). The gene is located downstream of a crotonase-like enoyl-CoA hydratase and upstream of an α-β hydrolase family esterase annotated to be

in the patatin phospholipase superfamily, suggesting that this protein is involved in fatty acid metabolism (35). However, while our paper was under review, Jendrossek and coworkers identified this protein in a bacterial two-hybrid screen using PhaC as the bait protein (49). From their studies, they hypothesized that it may be responsible for binding the granules to the bacterial nucleoid through its interactions with PhaC during cell segregation and granule formation. They renamed this protein PhaM. We will return to this protein in the discussion.

The most striking observation is the identification of the 20 kDa protein as PhaP1, the most abundant protein associated with PHB granules and calculated to cover 14–28% of the granule surface (25, 36). PhaP1 was eliminated as a priming factor because the presence of recombinantly purified PhaP1 was shown to increase the lag phase and decreases the rate of the linear phase in activity assays of PhaC with HBCoA (Figure S4), contrary to expectations for a priming factor. No other phasin proteins (PhaP2–5) were detected (28, 30). The identification of PhaP1 is supported by its absence in Strep2-PhaC$_{Re24h}$ purified from a $\Delta phaP1$ strain, Re2019 (Figure 3B, Lane 2). The absence of PhaP1 in the $\Delta phaP1$ strain was previously demonstrated using Western blots (24). The 20 kDa protein observed is biotin carboxyl carrier protein, likely co-purifying due to its affinity for the Strep-tactin resin. It is unclear why this protein is only observed in Strep2-PhaC$_{Re24h}$ isolated from the $\Delta phaP1$ strain. Finally a similar experiment, in which a Strep2-PhaC$_{Re24h}$ mutant with its active-site cysteine replaced with alanine (C319A), was purified from a C319A Strep2-PhaC$_{Re}$ strain, Re2017. It also failed to reveal PhaP1 (Figure 3B, Lane 3). Thus the detection of PhaP1 requires active PhaC, suggesting the importance of PHB for their co-purification.

Strep2-PhaC$_{Re24h}$ contains an active high molecular weight (HMW) fraction by SEC which contains PHB and PhaP1

An assay of Strep2-PhaC$_{Re24h}$ revealed the absence of a lag phase in CoA release (Figure 2), supporting the presence of a primed PhaC. Our previous in vitro studies revealed that primed PhaC is predominantly in the dimeric form (16). SEC, however, (Figure 4A) revealed in contrast to expectations, the presence of a HMW protein fraction based on its short retention time, as well as later eluting fractions containing dimeric and monomeric synthase, similar to Strep2-PhaC$_{Ec}$ (compare Figure 4A and 4C). Assays of the pooled HMW fractions exhibited no lag phase in CoA release and a specific activity of 35 ± 12 U/mg (Table S2). In contrast, the monomeric and dimeric forms of Strep2-PhaC$_{Re24h}$ exhibited lag phases, although they had similar specific activities, 30 ± 7 U/mg. SDS-PAGE analysis of the SEC fractions showed that PhaP1 is only associated with the HMW fraction (Figure 3A, lane 3). The small amount of PhaP1 in the dimer fraction (Figure 3A, lane 4) is due to the poor resolution of HMW and dimeric fractions. We note that an aggregate fraction is observed with Strep2-PhaC$_{Ec}$ (Figure 4C), also previously found in other purifications of PhaC from *E. coli* (15). In contrast with the HMW fraction observed with Strep2-PhaC$_{Re24h}$, however, the aggregate fraction of Strep2-PhaC$_{Ec}$ exhibits a low specific activity (~10 U/mg) compared with the dimer/monomer fractions and is comprised only of PhaC.

The C319A Strep2-PhaC$_{Re24h}$ had no HMW fraction (Figure S5), suggesting that the HMW fraction of Strep2-PhaC$_{Re24h}$ contained PHB. Analysis of all the SEC fractions from the experiment and mutant control for PHB via the crotonic acid assay (42), revealed its presence only in the HMW fraction. The observation of a soluble HMW fraction containing PHB, PhaC, and PhaP1 was unexpected and suggested that this fraction may result from precursors to granules or re-solubilized breakdown products of insoluble granules given its isolation at 24 h (Figure S1). This soluble, primed Strep2-PhaC$_{Re}$ could be providing insight about polymer initiation and granule genesis and thus we next attempted isolation of Strep2-

PhaC$_{Re}$ during maximum PHB production at 4 h (Figure S1), a time when granule initiation is more frequently occurring (25, 38).

Purification of Strep2-PhaC$_{Re4h}$

After 4 h growth in TSB medium, 83% of the total PHB in crude extracts is in the insoluble fraction, while 17% is soluble. Affinity chromatography of the soluble fraction resulted in reduced flow rate of the column suggesting some sample precipitation and significant activity loss in the column flow through and washes, suggesting inaccessibility of the Strep2 tag. A summary of the Strep2-PhaC$_{Re4h}$ purification is given in Table 3 and in Figure S6. Despite the low overall recovery of units, highly purified, active Strep2-PhaC$_{Re4h}$ (35 – 100 U/mg) was isolated.

SEC reveals a HMW fraction with Strep2-PhaC$_{Re4h}$, PhaP1, and PHB

SEC of Strep2-PhaC$_{Re4h}$ revealed a HMW fraction (Figure 4B) in addition to dimeric and monomeric PhaC. Some DNA co-purified with the HMW fraction despite incubation with DNase for 30 min during cell lysis (--- line Figure 4B, Figure S6). In light of recent data by Jendrossek and coworkers on PhaM, it is possible that DNA is present due to granule association with nucleoid (49). The HMW fraction isolated from SEC was assayed for activity; it exhibited no lag phase in CoA release and had a specific activity of 47 ± 13 U/mg. The pooled monomeric and dimeric fractions of Strep2-PhaC$_{Re4h}$ showed a lag phase and specific activity of 38 ± 8 U/mg (Figure 5, Table S2), similar to Strep2-PhaC$_{Re24h}$ and Strep2-PhaC$_{Ec}$. SDS-PAGE analysis revealed PhaP1 in both the unfractioned material and the HMW fraction (compare Figure 3C lanes 2 and 3, respectively). Quantitative Western blots of the HMW fraction from four different preparations gave a PhaP1/PhaC molar ratio from 2/1 to 4/1 (Figure S7). The 32 kDa (PhaM) (49), 60 kDa, and 75 kDa proteins were also observed (Figure 3C, lanes 2 and 3), while the 45 kDa protein was absent. Crotonic acid assays of the SEC fractions show PHB associated only with the HMW fraction. The recovery of PHB from the SEC column is 15–30%, likely associated with "granule" precipitation (Figure S6). The HMW and the dimeric/monomeric PhaC fractions suggest that in vivo, the elongation rate is faster than the initiation rate.

M$_w$ of PHB in Strep2-PhaC$_{Re4h}$

While the HMW fraction migrates as a large aggregate on the SEC matrix, we did not know how a PHB polymer or oligomers would affect the retention time of PhaC in this matrix. The size of the PHB has important implications in understanding the priming of PhaC and initiation of granule formation. To determine the size distribution of the PHB associated with purified Strep2-PhaC$_{Re4h}$, the PHB was extracted by refluxing in chloroform for 2 days. Crotonic acid assays revealed 74–100% of the total PHB was recovered. This material was analyzed by gel permeation chromatography (GPC) and gave a weight average molecular weight (M$_w$) of 350 kDa with a polydispersity index (PDI) of 1.7 relative to polystyrene standards. No attempt was made to isolate PHB from the HMW fraction of SEC due to the poor recovery from the column and the requirement for large amounts of material for GPC analysis. Control experiments using GPC to measure the M$_w$ of the PHB isolated from CHCl$_3$ extraction of the soluble and insoluble crude cell extract fractions showed M$_w$ of 320 kDa and 400 kDa and PDI of 1.7 and 2.1 respectively. Our results indicate that large M$_w$ PHB chains can be soluble, potentially providing important insight as to how PHB is packaged before it becomes an insoluble inclusion (3, 4).

Our GPC results indicate that this mutant strain produces PHB chains that are shorter than the isogenic wt strain grown under identical conditions (M$_w$ of 990 kDa with a PDI of 1.9), similar to our previous measurements made after 4 h growth in TSB medium in a shake flask (25). These results can be rationalized, as PhaC levels in the mutant strain are

substantially higher (35-fold) than the wt strain and previous studies in *E. coli* have shown that PHB molecular weight is decreased with increased synthase levels (50).

Finally, we also looked for oligomeric chains $(HB)_n$ in the extracted PHB from Strep2-PhaC$_{Re4h}$, which may be initially involved in priming the synthase. GPC, in which the refractive index signal is proportional to mass of PHB and independent of its chain length (51), failed to reveal any $(HB)_n$ oligomers. If short oligomers were present, they are <5% of the extracted material by mass given the limit of detection by this method.

Ratios of Strep2-PhaC$_{Re4h}$/PhaP1/PHB

Our previous studies of the wt strain showed that the molar ratio of PhaC/PhaP1/PHB in whole cells, assuming PhaC and PhaP1 are monomers, was ~0.01/1/1 after 4 h growth in TSB medium (25). The observation of 1/1 PHB to PhaP1 suggested an important role for PhaP1 mechanistically. The low PhaC to PHB ratio of 0.01/1 suggested that the PhaC can reinitiate polymer formation after chain termination when PHB chains of defined length are generated (18, 25). Using the M_w of 350 kDa and the amounts of PHB and protein determined by crotonic acid assays and quantitative Western blots respectively, the molar ratio of Strep2-PhaC/PhaP1/PHB was calculated to range from 1/4/1 to 3/9/1 in the HMW fraction (based on 3 different preparations) compared to 0.1/0.6/1 in Re2018 mutant whole cells grown for 4 h in TSB (Table 4). In whole cells from the Re2018 strain, as with the wt strain, the ratio of PhaP1 to PHB is ~1/1. However, in the HMW fraction, the ratio is increased to 4–9/1. Although there are several explanations for this observation, we suggest that in the HMW fraction, several PhaP1 molecules associate with a large molecular weight PHB chain to form a structure to facilitate polymer solubility and that this PhaC•PhaP1•PHB complex may be the initial, nucleating species for granule formation. With time, as more and more HB units are added to this species, the PhaP1/PHB ratio decreases from 4–9/1 to 1/1 and the Strep2-PhaC/PHB ratio decreases from 1–3/1 to 0.1/1 (Table 4). The ratio of Strep2-PhaC/PHB in the HMW fraction of 1–3/1 is within error of the stoichiometry of one PHB chain per PhaC dimer observed when the synthase is artificially primed in vitro (16). This ratio thus suggests that the HMW fraction contains primed synthase in which the primer is $(HB)_n$ where n is large, but ≤ ~4000 (350 kDa). A large PHB chain serving as the primer is consistent with the elongation rate of PHB formation being much greater than the initiation rate demonstrated in vitro (8, 18). The co-purification of PhaC, PhaP1, and PHB and changes in their ratios provide the basis for our modified micelle model for granule genesis described subsequently (Figure 6A2).

Discussion

In vitro assays of all synthases examined to date have elongation rates for PHB formation that are much faster than the initiation rates (8, 10–13, 18, 52). This observation has made it challenging to study the initiation or priming process and to formulate a model for granule genesis that avoids cellular toxicity associated with non-specific hydrophobic binding of cellular components to the PHB. We therefore undertook a search for a protein(s) in *R. eutropha* that might be involved in increasing the rate of initiation by a priming process similar to our previous observations with artificial primers (Figure 1, $(HB)_3CoA$, sTCoA) (16). Since PhaC has never been isolated from its host organism due to its prevalence on insoluble inclusions (8), our approach was to engineer a strain of *R. eutropha* to express an affinity tagged PhaC. The strategy was successful and a highly purified Strep2-tagged PhaC$_{Re}$ was isolated from the native organism *R. eutropha* for the first time (Figure 3).

Studies with this PhaC have allowed a number of important observations to be made about the initiation and elongation steps of PHB polymerization. First, the activity assays with Strep2-PhaC$_{Re}$ showed NO lag phase in CoA production, distinct from recombinantly

expressed PhaC$_{Ec}$, suggesting that PhaC$_{Re}$ is primed. GPC analysis of the PHB isolated with PhaC$_{Re}$ suggests that it is primed by (HB)$_n$, where n is large. Thus while our initial efforts were focused on the identification of a "protein" primer, our studies reveal that the primer is likely (HB)$_n$ itself (53). Second, the SEC analysis revealed that the purified material contained not only the soluble HMW complex, but also, unmodified dimeric/monomeric PhaC. The observation of two populations of PhaC suggests that the polymer elongation rate is much faster than the initiation rate as previously observed in vitro (8, 18). Thus we are still left with the issue of how granule genesis is controlled.

We believe that insight into this mechanism has been provided by the unexpected isolation of soluble PhaC in a complex with PhaP1 and large molecular weight PHB chains. Based on the mole ratios of these species within the complex, a modified micelle model for granule genesis (Figure 6A2) is presented. While the HMW complex is kinetically competent at PHB production, demonstration that it is on pathway to insoluble granules will require additional experimental approaches.

Models for granule genesis

In vitro studies have shown that granules can be generated with HBCoA and PhaC only, although they are much larger in size and the PHB is higher in molecular weight than granules found in vivo (54–56). Thus granules can form by self-assembly. Therefore, it is not surprising that a self-assembly micelle model was the first proposed mechanism for granule genesis (57). However, recently, a membrane budding model (4, 58, 59) and a scaffolding model (25, 60) have also been considered as alternatives.

Our studies have led us now to favor a modified micelle model. It differs from the original micelle model (Figure 6A1) where (HB)$_n$ oligomers (n is small) covalently attached to PhaC, were proposed to aggregate to form a micelle-like structure in the absence of PhaP1 (19, 20). This model requires a controlled elongation rate so that short PHB chains have sufficient time to form the micelle structure (19, 20). Our observations that the elongation rate is faster than the initiation rate in vivo and that PhaP1 levels are relatively high at an early stage of granule genesis have led to our modified micelle model (Figure 6A2). In our model, the initial nucleating species consists of a PhaC dimer covalently attached to one PHB chain ((HB)$_n$ where n is large) to which several PhaP1s (4–9 monomer units) are associated to maintain solubility (Figure 6A2). Exposed hydrophobic patches of (HB)$_n$ in this species allow fusion with similar nucleating species and give rise to a soluble granule precursor. A mixture of the nucleating species and soluble granule precursors is proposed to comprise the HMW fraction of Strep2-PhaC$_{Re4h}$. The molar ratio of 1–3/1 PhaC/PHB chain in the HMW fraction (Table 4) and the lack of a lag phase in CoA release are consistent with our in vitro studies on primed synthase, with one PHB chain per dimeric synthase (16). The phase transition from a soluble to an insoluble granule requires addition of HB units and re-initiation of polymer formation. Recall that mature granules found in Re2018 and wt whole cells have many more PHB chains than PhaC molecules (Table 4, ~100/1 in wt and ~10/1 in Re2018 grown in TSB) (25). During this phase transition, the molar ratio of PhaP1/PHB decreases, eventually reaching the level of 0.6/1 in Re2018, similar to the ~1/1 in wt cells under TSB growth conditions (25). Finally, other proteins associated with PHB homeostasis (PhaR and PhaZs) were not observed with the purified Strep2-PhaC$_{Re4h}$. Since these proteins have previously been shown to associate with mature PHB granules either by insoluble granule isolation or immunogold labeling (28, 30, 31, 33), they are proposed to bind to the granule exterior as the ratio of PhaP1/PHB decreases to 1/1 and more exposed PHB becomes accessible to the granule surface.

A second model for granule genesis, the membrane budding model, is based on the analogies with lipid bodies and their biogenesis in eukaryotic systems (4, 61). In this model

(Figure 6B), PhaC and PhaP1 bind to the inner leaflet of the plasma membrane with PHB chains from PhaC extended into the membrane. The PHB granules subsequently bud from the membrane, with a monolayer of phospholipid and PhaC and PhaP1 residing on the granule surface. Previous fluorescence studies have been interpreted to support this model (58, 59). In the past year, however, a number of observations have been published which suggest that this model is unlikely. First, our examination of recent microarray data reporting changes in gene expression associated with PHB production, revealed down regulation of the biosynthetic pathways associated with phospholipids found in *R. eutropha* membranes: phosphatidylethanolamine, phosphatidylglycerol, and cardiolipin (27, 29). This is the opposite of expectations for the budding model in which each granule is covered with a lipid monolayer. Second, cryoelectron tomography has recently been used to examine granule surfaces and localization in *R. eutropha* during PHB production in nitrogen limited growth medium (38). These studies revealed discontinuous surface coverage of the granules inconsistent with a lipid monolayer. No granules (of 450 examined) were budding from the membrane. Finally, our observation in this paper of the soluble PhaC/PhaP1/PHB complex is at odds with a membrane budding model as a lipid coated PHB would likely be insoluble. Thus in the case of *R. eutropha*, the membrane budding model for granule genesis is unlikely.

A scaffolding model (Figure 6C) (where the scaffold was an unspecified macromolecule) was previously proposed based on negative staining TEM of *R. eutropha* at early stages of granule genesis during growth in TSB medium and in nitrogen limited medium (25, 60). The granules appeared to be associated with "dark-stained features" in the center of the cells, which we now believe to be the bacterial nucleoid. A nucleoid scaffolding model (Figure 6C) recently became more interesting as Jendrossek and coworkers, using *R. eutropha* PhaC as bait in a screen for protein-protein interactions via a two-hybrid method (49), identified an interaction with a previously uncharacterized *R. eutropha* protein, which they designated PhaM (26.6 kDa). This protein has PAKKA-like motifs at its C-terminus, proposed in other systems to be involved in "non-specific" DNA binding (62, 63). From a variety of additional studies, they proposed that PHB granules bind to nucleoid via this protein during granule formation and cell segregation. In the latter case, this binding would provide a mechanism for equal segregation of granules among daughter cells (49, 62). It is interesting to note that the 32 kDa protein that co-purified with Strep2-PhaC$_{Re}$ at both 4 h and 24 h is PhaM. From our biochemical and biological studies above, the modified micelle model for granule formation (Figure 6A2) could be integrated with a scaffolding model where the scaffold would be bacterial nucleoid. Thus a nucleoid scaffolding model cannot at present be distinguished from a random cytoplasmic micelle model.

Summary

The results presented in this study provide the first glimpse into the initiation process of granule formation in *R. eutropha*. The studies suggest that PhaC is primed by rapid acylation and elongation of its active site cysteine by HBCoA, in accord with in vitro studies where the elongation rate is much faster than the initiation rate (8, 18). The soluble HMW complex of PhaC/PhaP1 and high molecular weight PHB is capable of adding HB units to the primed PhaC in a kinetically competent fashion. The molar ratios of these species relative to those observed on mature granules have led to our modified micelle model for granule genesis that provides the basis for future studies.

Supplementary Material

Refer to Web version on PubMed Central for supplementary material.

Acknowledgments

Abbreviations and Textual Footnotes

PHB	polyhydroxybutyrate
PHV	polyhydroxyvalerate
Strep2-PhaC$_{Ec}$	*N*-terminal-Strep2-(G$_4$S)$_3$-tagged PhaC purified from *E. coli*
N-terminal Strep2-PhaC$_{Re}$	Strep2-(G$_4$S)$_3$-tagged PhaC purified from *R. eutropha*
Strep2-PhaC$_{Re24h}$	Strep2-PhaC purified from *R. eutropha* culture after 24 h of growth in TSB medium
Strep2-PhaC$_{Re4h}$	Strep2-PhaC purified from *R. eutropha* culture after 4 h of growth in TSB medium
SEC	size exclusion chromatography
HMW	high molecular weight
HBCoA	3-hydroxybutyryl-CoA
(HB)$_n$	oligomers of 3-hydroxybutyrate of length n
gent	gentamicin
kan	kanamycin
amp	ampicillin
sTCoA	an analog of (HB)$_3$-CoA in which the terminal HO group is replaced with a H
TSB	tryptic soy broth
TAE	Tris-Acetate-EDTA buffer
IPTG	isopropyl-β-thiogalactoside
OD$_{600}$	optical density at 600 nm
RT	room temperature
cdw	cell dry weight
A$_{280}$	absorbance at 280 nm
TEM	transmission electron microscopy

References

1. Peoples OP, Sinskey AJ. Poly-β-hydroxybutyrate (PHB) biosynthesis in *Alcaligenes eutrophus* H16. Identification and characterization of the PHB polymerase gene (*phbC*). J Biol Chem. 1989; 264:15298–15303. [PubMed: 2670936]

2. Steinbüchel A, Valentin HE. Diversity of polyhydroxyalkanoic acids. FEMS Microbiol Lett. 1995; 128:219–228.

3. Stubbe J, Tian J. Polyhydroxyalkanoate (PHA) homeostasis: The role of PHA synthase. Nat Prod Rep. 2003; 20:445–457. [PubMed: 14620841]

4. Stubbe J, Tian J, He A, Sinskey AJ, Lawrence AG, Liu P. Nontemplate-dependent polymerization processes: Polyhydroxyalkanoate synthases as a paradigm. Annu Rev Biochem. 2005; 74:433–480. [PubMed: 15952894]

5. Sudesh K, Abe H, Doi Y. Synthesis, structure, and properties of polyhydroxyalkanoates: Biological polyesters. Prog Polym Sci. 2000; 25:1503–1555.

6. Keshavarz T, Roy I. Polyhydroxyalkanoates: Bioplastics with a green agenda. Curr Opin Microbiol. 2010; 13:321–326. [PubMed: 20227907]

7. Peoples OP, Snell KD. PHA bioplastic: A value-added coproduct for biomass biorefineries. Biofuels, Bioprod Biorefin. 2009; 3:456–467.

8. Gerngross TU, Snell KD, Peoples OP, Sinskey AJ, Csuhai E, Masamune S, Stubbe J. Overexpression and purification of the soluble polyhydroxyalkanoate synthase from *Alcaligenes eutrophus*: Evidence for a required posttranslational modification for catalytic activity. Biochemistry. 1994; 33:9311–9320. [PubMed: 8049232]

9. Liebergesell M, Sonomoto K, Madkour M, Mayer F, Steinbüchel A. Purification and characterization of the poly(hydroxyalkanoic acid) synthase from *Chromatium vinosum* and localization of the enzyme at the surface of poly(hydroxyalkanoic acid) granules. Eur J Biochem. 1994; 226:71–80. [PubMed: 7957260]

10. Qi Q, Steinbüchel A, Rehm BHA. In vitro synthesis of poly(3-hydroxydecanoate): purification and enzymatic characterization of type II polyhydroxyalkanoate synthases PhaC1 and PhaC2 from *Pseudomonas aeruginosa*. Appl Microbiol Biotechnol. 2000; 54:37–43. [PubMed: 10952003]

11. Hai T, Hein S, Steinbüchel A. Multiple evidence for widespread and general occurrence of type-III PHA synthases in cyanobacteria and molecular characterization of the PHA synthases from two thermophilic cyanobacteria: *Chlorogloeopsis fritschii* PCC 6912 and *Synechococcus sp* strain MA19. Microbiology. 2001; 147:3047–3060. [PubMed: 11700355]

12. Zhang S, Kolvek S, Goodwin S, Lenz RW. Poly(hydroxyalkanoic acid) biosynthesis in *Ectothiorhodospirashaposhnikovii*: Characterization and reactivity of a type III PHA synthase. Biomacromolecules. 2004; 5:40–48. [PubMed: 14715006]

13. Bhubalan K, Chuah JA, Shozui F, Brigham CJ, Taguchi S, Sinskey AJ, Rha C, Sudesh K. Characterization of the highly active polyhydroxyalkanoate synthase of *Chromobacterium sp* strain USM2. Appl Environ Microbiol. 2011; 77:2926–2933. [PubMed: 21398494]

14. Jia Y, Yuan W, Wodzinska J, Park C, Sinskey AJ, Stubbe J. Mechanistic studies on class I polyhydroxybutyrate (PHB) synthase from *Ralstonia eutropha*: Class I and III synthases share a similar catalytic mechanism. Biochemistry. 2001; 40:1011–1019. [PubMed: 11170423]

15. Yuan W, Jia Y, Tian J, Snell KD, Müh U, Sinskey AJ, Lambalot RH, Walsh CT, Stubbe J. Class I and III polyhydroxyalkanoate synthases from *Ralstonia eutropha* and *Allochromatium vinosum*: Characterization and substrate specificity studies. Arch Biochem Biophys. 2001; 394:87–98. [PubMed: 11566031]

16. Wodzinska J, Snell KD, Rhomberg A, Sinskey AJ, Biemann K, Stubbe J. Polyhydroxybutyrate synthase: Evidence for covalent catalysis. J Am Chem Soc. 1996; 118:6319–6320.

17. Zhang S, Yasuo T, Lenz RW, Goodwin S. Kinetic and mechanistic characterization of the polyhydroxybutyrate synthase from *Ralstonia eutropha*. Biomacromolecules. 2000; 1:244–251. [PubMed: 11710107]

18. Tian J, Sinskey AJ, Stubbe J. Class III polyhydroxybutyrate synthase: Involvement in chain termination and reinitiation. Biochemistry. 2005; 44:8369–8377. [PubMed: 15938626]

19. Griebel R, Smith Z, Merrick JM. Metabolism of poly-beta-hydroxybutyrate. I Purification, composition, and properties of native poly-beta-hydroxybutyrate granules from. Bacillus megaterium Biochemistry. 1968; 7:3676–3681.

20. Gerngross TU, Reilly P, Stubbe J, Sinskey AJ, Peoples OP. Immunocytochemical analysis of poly-beta-hydroxybutyrate (PHB) synthase in *Alcaligenes eutrophus* H16: Localization of the synthase enzyme at the surface of PHB granules. J Bacteriol. 1993; 175:5289–5293. [PubMed: 8349571]

21. Wieczorek R, Pries A, Steinbüchel A, Mayer F. Analysis of a 24-kilodalton protein associated with the polyhydroxyalkanoic acid granules in *Alcaligenes eutrophus*. J Bacteriol. 1995; 177:2425–2435. [PubMed: 7730274]

22. Shaw GL, Melby MK, Horowitz DM, Keeler J, Sanders JK. Nuclear magnetic resonance relaxation studies of poly(hydroxybutyrate) in whole cells and in artificial granules. Int J Biol Macromol. 1994; 16:59–63. [PubMed: 8011588]

23. York GM, Junker BH, Stubbe JA, Sinskey AJ. Accumulation of the PhaP phasin of *Ralstonia eutropha* is dependent on production of polyhydroxybutyrate in cells. J Bacteriol. 2001; 183:4217–4226. [PubMed: 11418562]

24. York GM, Stubbe J, Sinskey AJ. New insight into the role of the PhaP phasin of *Ralstonia eutropha* in promoting synthesis of polyhydroxybutyrate. J Bacteriol. 2001; 183:2394–2397. [PubMed: 11244085]

25. Tian J, He A, Lawrence AG, Liu P, Watson N, Sinskey AJ, Stubbe J. Analysis of transient polyhydroxybutyrate production in *Wautersia eutropha* H16 by quantitative Western analysis and transmission electron microscopy. J Bacteriol. 2005; 187:3825–3832. [PubMed: 15901707]

26. Lawrence AG, Schoenheit J, He A, Tian J, Liu P, Stubbe J, Sinskey AJ. Transcriptional analysis of *Ralstonia eutropha* genes related to poly-(R)-3-hydroxybutyrate homeostasis during batch fermentation. Appl Microbiol Biotechnol. 2005; 68:663–672. [PubMed: 15924243]

27. Horowitz DM, Sanders JKM. Amorphous, biomimetic granules of polyhydroxybutyrate: Preparation, characterization, and biological implications. J Am Chem Soc. 1994; 116:2695–2702.

28. Pötter M, Müller H, Reinecke F, Wieczorek R, Fricke F, Bowien B, Friedrich B, Steinbüchel A. The complex structure of polyhydroxybutyrate (PHB) granules: Four orthologous and paralogous phasins occur in *Ralstonia eutropha*. Microbiology. 2004; 150:2301–2311. [PubMed: 15256572]

29. Brigham CJ, Budde CF, Holder JW, Zeng Q, Mahan AE, Rha C, Sinskey AJ. Elucidation of beta-oxidation pathways in *Ralstonia eutropha* H16 by examination of global gene expression. J Bacteriol. 2010; 192:5454–5464. [PubMed: 20709892]

30. Pfeiffer D, Jendrossek D. Interaction between poly(3-hydroxybutyrate) granule-associated proteins as revealed by two-hybrid analysis and identification of a new phasin in *Ralstonia eutropha*. Microbiology. 2011; 157:2795–2807. [PubMed: 21737497]

31. Pötter M, Madkour MH, Mayer F, Steinbüchel A. Regulation of phasin expression and polyhydroxyalkanoate (PHA) granule formation in *Ralstonia eutropha* H16. Microbiology. 2002; 148:2413–2426. [PubMed: 12177335]

32. York GM, Stubbe J, Sinskey AJ. The *Ralstonia eutropha* PhaR protein couples synthesis of the PhaP phasin to the presence of polyhydroxybutyrate in cells and promotes polyhydroxybutyrate production. J Bacteriol. 2002; 184:59–66. [PubMed: 11741844]

33. Saegusa H, Shiraki M, Kanai C, Saito T. Cloning of an intracellular poly[D(−)-3-hydroxybutyrate] depolymerase gene from *Ralstonia eutropha* H16 and characterization of the gene product. J Bacteriol. 2001; 183:94–100. [PubMed: 11114905]

34. York GM, Lupberger J, Tian J, Lawrence AG, Stubbe J, Sinskey AJ. *Ralstonia eutropha* H16 encodes two and possibly three intracellular poly[D-(−)-3-hydroxybutyrate] depolymerase genes. J Bacteriol. 2003; 185:3788–3794. [PubMed: 12813072]

35. Pohlmann A, Fricke WF, Reinecke F, Kusian B, Liesegang H, Cramm R, Eitinger T, Ewering C, Pötter M, Schwartz E, Strittmatter A, Voß I, Gottschalk G, Steinbüchel A, Friedrich B, Bowien B. Genome sequence of the bioplastic-producing "Knallgas" bacterium *Ralstonia eutropha* H16. Nat Biotechnol. 2006; 24:1257–1262. [PubMed: 16964242]

36. Neumann L, Spinozzi F, Sinibaldi R, Rustichelli F, Pötter M, Steinbüchel A. Binding of the major phasin, PhaP1, from *Ralstonia eutropha* H16 to poly(3-hydroxybutyrate) granules. J Bacteriol. 2008; 190:2911–2919. [PubMed: 18223073]

37. Haywood GW, Anderson AJ, Dawes EA. The importance of PHB-synthase substrate specificity in polyhydroxyalkanoate synthesis by *Alcaligenes eutrophus*. FEMS Microbiol Lett. 1989; 57:1–6.

38. Beeby, M.; Cho, M.; Stubbe, J.; Jensen, GJ. [accessed Dec 16, 2011] Growth and localization of polyhydroxybutyrate granules in *Ralstonia eutropha*. J Bacteriol. 2011. [Online early access]Published online: Dec 16, 2011. http://jb.asm.org/content/early/2011/12/13/JB.06125-11

39. Bradford MM. A rapid and sensitive method for the quantitation of microgram quantities of protein utilizing the principle of protein-dye binding. Anal Biochem. 1976; 72:248–254. [PubMed: 942051]

40. Budde CF, Riedel SL, Willis LB, Rha C, Sinskey AJ. Production of poly(3-hydroxybutyrate-co-3-hydroxyhexanoate) from plant oil by engineered *Ralstonia eutropha* strains. Appl Environ Microbiol. 2011; 77:2847–2854. [PubMed: 21398488]

41. Quandt J, Hynes MF. Versatile suicide vectors which allow direct selection for gene replacement in gram-negative bacteria. Gene. 1993; 127:15–21. [PubMed: 8486283]

42. Karr DB, Waters JK, Emerich DW. Analysis of poly-beta-hydroxybutyrate in *Rhizobium japonicum* bacteroids by ion-exclusion high-pressure liquid chromatography and UV detection. Appl Environ Microbiol. 1983; 46:1339–1344. [PubMed: 16346443]

43. Harlow, E.; Lane, D. Antibodies : A laboratory manual. Cold Spring Harbor Laboratory Press; Plainview, NY: 1988.

44. Scopes RK, Smith JA. Analysis of proteins. Curr Protoc Mol Biol. 2010; 90:10.10.11–10.10.23.

45. Tian, J. Chemistry. Massachusetts Institute of Technology; Cambridge, MA: 2005. Mechanistic investigation of polyhydroxybutyrate (PHB) synthases and elucidation of PHB biosynthesis and degradation process in *Wautersia eutropha* H16; p. 345

46. Terpe K. Overview of tag protein fusions: From molecular and biochemical fundamentals to commercial systems. Appl Microbiol Biotechnol. 2003; 60:523–533. [PubMed: 12536251]

47. Budde CF, Mahan AE, Lu J, Rha C, Sinskey AJ. The roles of multiple acetoacetyl-CoA reductases in polyhydroxybutyrate biosynthesis in *Ralstonia eutropha* H16. J Bacteriol. 2010; 192:5319–5328. [PubMed: 20729355]

48. Schubert T, Lenz O, Krause E, Volkmer R, Friedrich B. Chaperones specific for the membrane-bound [NiFe]-hydrogenase interact with the Tat signal peptide of the small subunit precursor in *Ralstonia eutropha* H16. Mol Microbiol. 2007; 66:453–467. [PubMed: 17850259]

49. Pfeiffer D, Wahl A, Jendrossek D. Identification of a multifunctional protein, PhaM, that determines number, surface to volume ratio, subcellular localization and distribution to daughter cells of poly(3-hydroxybutyrate), PHB, granules in *Ralstonia eutropha* H16. Mol Microbiol. 2011; 82:936–951. [PubMed: 22023320]

50. Sim SJ, Snell KD, Hogan SA, Stubbe J, Rha C, Sinskey AJ. PHA synthase activity controls the molecular weight and polydispersity of polyhydroxybutyrate in vivo. Nat Biotechnol. 1997; 15:63–67. [PubMed: 9035108]

51. Bürger HM, Müller HM, Seebach D, Börnsen KO, Schär M, Widmer HM. Matrix-assisted laser desorption and ionization as a mass spectrometric tool for the analysis of poly[(R)-3-hydroxybutanoates]. Comparison with gel permeation chromatography. Macromolecules. 1993; 26:4783–4790.

52. Jia Y, Kappock TJ, Frick T, Sinskey AJ, Stubbe J. Lipases provide a new mechanistic model for polyhydroxybutyrate (PHB) synthases: Characterization of the functional residues in *Chromatium vinosum* PHB synthase. Biochemistry. 2000; 39:3927–3936. [PubMed: 10747780]

53. A recent report by Kudo and coworkers suggested that succinyl-CoA functions as a primer [Yamanaka K, Kimura Y, Aoki T, Kudo T. End-group analysis of bacterially produced poly(3-hydroxybutyrate): Discovery of succinate as the polymerization starter. Macromolecules. 2009; 42:4038–4046.]. In our hands, however, succinyl-CoA does not acylate PhaC and has no effect on the lag phase of CoA release with HBCoA.

54. Gerngross TU, Martin DP. Enzyme-catalyzed synthesis of poly[(R)-(−)-3-hydroxybutyrate]: Formation of macroscopic granules in vitro. Proc Natl Acad Sci USA. 1995; 92:6279–6283. [PubMed: 7603982]

55. Hiraishi T, Kikkawa Y, Fujita M, Normi YM, Kanesato M, Tsuge T, Sudesh K, Maeda M, Doi Y. Atomic force microscopic observation of in vitro polymerized poly[(R)-3-hydroxybutyrate]: Insight into possible mechanism of granule formation. Biomacromolecules. 2005; 6:2671–2677. [PubMed: 16153105]

56. Nobes GAR, Jurasek L, Marchessault RH, Martin DP, Putaux JL, Chanzy H. Growth and kinetics of in vitro poly([R]-(−)-3-hydroxybutyrate) granules interpreted as particulate polymerization with coalescence. Macromol Rapid Commun. 2000; 21:77–84.

57. Ellar D, Lundgren DG, Okamura K, Marchessault R. Morphology of poly-β-hydroxybutyrate granules. J Mol Biol. 1968; 35:489–502. [PubMed: 4970600]

58. Jendrossek D. Fluorescence microscopical investigation of poly(3-hydroxybutyrate) granule formation in bacteria. Biomacromolecules. 2005; 6:598–603. [PubMed: 15762619]

59. Jendrossek D. Polyhydroxyalkanoate granules are complex subcellular organelles (carbonosomes). J Bacteriol. 2009; 191:3195–3202. [PubMed: 19270094]

60. Tian J, Sinskey AJ, Stubbe J. Kinetic studies of polyhydroxybutyrate granule formation in *Wautersia eutropha* H16 by transmission electron microscopy. J Bacteriol. 2005; 187:3814–3824. [PubMed: 15901706]

61. Parthibane V, Rajakumari S, Venkateshwari V, Iyappan R, Rajasekharan R. Oleosin is bifunctional enzyme that has both monoacylglycerol acyltransferase and phospholipase activities. J Biol Chem. 2012; 287:1946–1954. [PubMed: 22128159]

62. Galán B, Dinjaski N, Maestro B, de Eugenio LI, Escapa IF, Sanz JM, García JL, Prieto MA. Nucleoid-associated PhaF phasin drives intracellular location and segregation of polyhydroxyalkanoate granules in *Pseudomonas putida* KT2442. Mol Microbiol. 2011; 79:402–418. [PubMed: 21219460]

63. Kasinsky HE, Lewis JD, Dacks JB, Ausio J. Origin of H1 linker histones. FASEB J. 2001; 15:34–42. [PubMed: 11149891]

64. Simon S, Priefer T, Pühler A. A broad host range mobilization system for in vivo genetic engineering: Transposon mutagenesis in Gram negative bacteria. Nat Biotechnol. 1983; 1:784–791.

Figure 1.
Structure of (HB)$_3$CoA and sTCoA. Primers for in vitro production of PHB by PhaC$_{Ec}$.
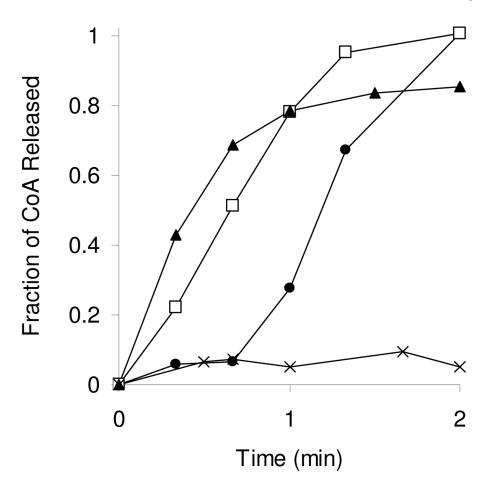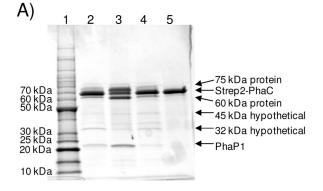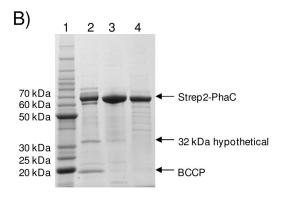(HB)$_3$CoA, X=OH. sTCoA, X=H.

Figure 2.
Time course of CoA release from HBCoA at 30 °C catalyzed by Strep2-tagged synthases purified from *R. eutropha* at 24 h and 4 h TSB growth and from *E. coli*. The reaction mixtures for Strep2-PhaC$_{Re24h}$ (□), Strep2-PhaC$_{Ec}$ (●), and C319A Strep2-PhaC$_{Re}$ (×) contain 60 nM enzyme and 750 μM HBCoA. The reaction mixture for Strep2-PhaC$_{Re4h}$ (▲) contains 60 nM enzyme and 600 μM HBCoA. HBCoA concentrations used in the assays are well above the K_m (100 μM) (17).
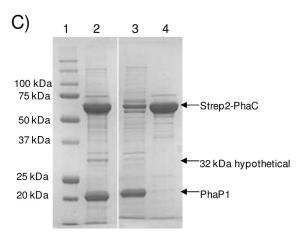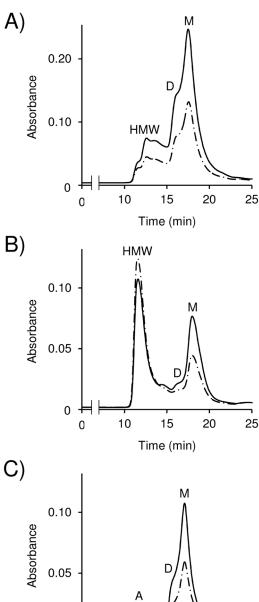
Figure 3.
SDS-PAGE gels of unfractionated, SEC purified HMW, dimer, and monomer fractions of the Strep2-tagged synthases purified from *R. eutropha* strains at 24 h and 4 h TSB growth and from *E. coli*. A) Gradient SDS-PAGE (4–15%) gel of Strep2-PhaC$_{Re24h}$ SEC fractions. Lane 1, Molecular weight standards; Lane 2, Unfractionated Strep2-PhaC$_{Re24h}$; Lane 3, HMW fraction; Lane 4, Dimer fraction; Lane 5, Monomer fraction. B) Gradient SDS-PAGE (4–15%) gel of Strep2-PhaC purified from a Δ*phaP1 R. eutropha* strain, C319A Strep2-PhaC purified from a C319A-*strep2-phaC R. eutropha* strain, and Strep2-PhaC purified from *E. coli* as controls. Lane 1, Molecular weight standards; Lane 2, Strep2-PhaC purified from a Δ*phaP1 R. eutropha* strain; Lane 3, C319A Strep2-PhaC$_{Re}$; Lane 4, Strep2-PhaC$_{Ec}$. C) SDS-PAGE (10%) gel of Strep2-PhaC$_{Re4h}$ SEC fractions. Lane 1, Molecular weight standards; Lane 2, Unfractionated Strep2-PhaC$_{Re4h}$; Lane 3, HMW fraction; Lane 4, Dimer/

monomer fraction. Strep2-PhaC, PhaP1, biotin carboxyl carrier protein (BCCP), and co-purifying 32 kDa, 45 kDa, 60 kDa, and 70 kDa proteins identified by Edman sequencing are labeled accordingly.

Figure 4.
Bio-Sil SEC250-5 size exclusion chromatography of Strep2-tagged synthases purified from *R. eutropha* at 24 h and 4 h TSB growth and from *E. coli*. A) SEC of Strep2-PhaC$_{Re24h}$. B) SEC of Strep2-PhaC$_{Re4h}$. C) SEC of Strep2-PhaC$_{Ec}$. Peaks D and M are the dimer and monomer fractions respectively. Peaks labeled HMW are the high molecular weight fractions containing PHB. Peak A is a protein aggregate, containing no PHB. Solid line, absorbance at 280 nm; dotted line, absorbance at 260 nm.
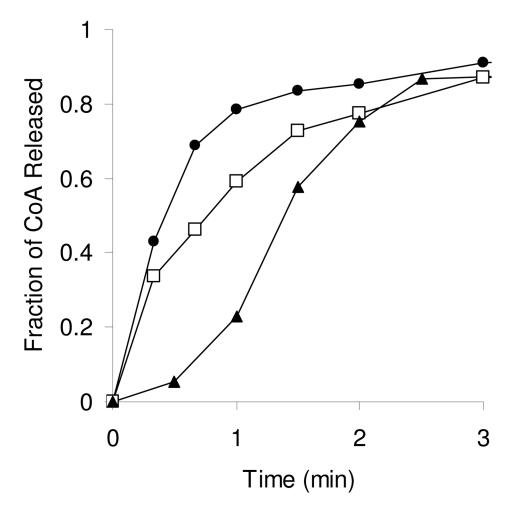
Figure 5.
Time course of CoA release from HBCoA at 30 °C catalyzed by unfractionated Strep2-PhaC$_{Re4h}$ and HMW and dimer/monomer SEC fractions of Strep2-PhaC$_{Re4h}$. The reaction mixtures contain 600 μM HBCoA and either 60 nM unfractionated Strep2-PhaC$_{Re4h}$ (●), 60 nM HMW fraction (□), or 80 nM dimer/monomer fraction (▲). Assays for the unfractionated, HMW, and dimer/monomer fractions of Strep2-PhaC$_{Re24h}$ are similar to the assays for the respective Strep2-PhaC$_{Re4h}$ fractions.

A2) Modified micelle model:

Nucleating species

PhaC dimer

Full-length PHB chain

PhaP1

Fusion, HBCoA

A1) Original micelle model:

Micelle-like structure

PhaC dimer

PHB oligomers

HBCoA, PhaP1

Soluble precursor

Full-length PHB chains

HBCoA
Other PhaPs ○
PhaR ■
PhaZs ▲

Re-initiation, Phase transition

Insoluble PHB granule

B) Membrane model

Inner Membrane   Outer Membrane

PHB chains

Phospholipid monolayer

PhaP1

PhaC dimer

HBCoA, PhaP1

Budding

PHB granule

C) Scaffolding model

Scaffold

Membrane

PhaC dimer   PhaP1

HBCoA, PhaP1

PHB chains

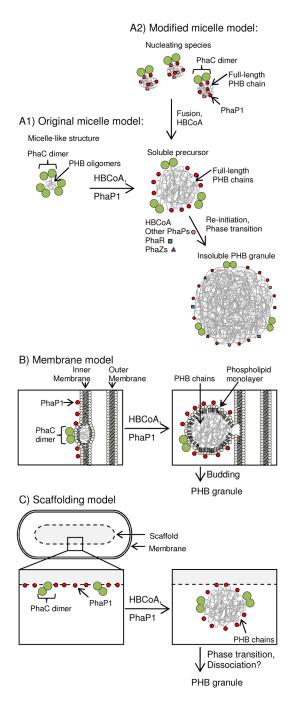Phase transition, Dissociation?

PHB granule

Figure 6.
Models for granule formation. PhaC and PhaP1 are represented as green and red spheres respectively. PhaP1 is represented as a monomer in the figures, but may have higher oligomeric states (i.e. trimer). A) Micelle models for granule formation. In the original micelle model (A1), several short PHB chains covalently attached to PhaC associate to form an initial micelle-like structure, to which PhaP1 later binds in a soluble granule precursor. The original micelle model assumes that the polymer elongation rate is controlled relative to the initiation rate to allow for short PHB chains to aggregate. In the modified micelle model (A2), single, full-length PHB chains covalently attached to PhaC associate with PhaP1 early on in a nucleating species to allow for the polymer elongation rate to be faster than the

initiation rate. Several nucleating species fuse together to form a soluble granule precursor. The soluble granule precursor later undergoes a phase transition to form the mature granule. B) Membrane model. In this model, PhaC and PhaP1 bind to the inner leaflet of the inner membrane with PhaC synthesizing PHB chains into the membrane. Eventually, the nascent granule buds from the membrane with PhaC, PhaP1, and a phospholipid monolayer found at the surface. C) Scaffolding model. In this model, PhaC and PhaP1 interact with a protein and/or DNA scaffold in the cytoplasm of the cell, which serves as the starting point for granule formation.

Table 1

Strains and Plasmids

Strain	Genotype	Reference
Ralstonia eutropha		
Re1034	H16, $\Delta phaC$	(23)
Re1052	H16, $\Delta phaP1$	(24)
Re1053	Re1034, $\Delta phaP1$	This work
Re2016	Re1034 w/ *N*-terminal (His)$_6$ tagged *phaC* gene inserted into $\Delta phaC$ locus	This work
Re2018	Re1034 with *N*-terminal Strep2 tagged *phaC* gene containing a (G$_4$S)$_3$ linker inserted into $\Delta phaC$ locus	This work
Re2019	Re1053 with *N*-terminal Strep2 tagged *phaC* gene containing a (G$_4$S)$_3$ linker inserted into $\Delta phaC$ locus	This work
Re2017	Re1034 with *N*-terminal Strep2 tagged *phaC* C319A mutant gene containing a (G$_4$S)$_3$ linker inserted into $\Delta phaC$ locus	This work
Escherichia coli		
BL21(DE3)	Strain for protein expression from pET-based vectors.	Novagen
S17-1	Strain for conjugative transfer of plasmids into *R. eutropha*	(64)

Plasmid	Description	Reference
pET51b	*N*-terminal Strep2-tag cloning plasmid, confers amp resistance	Novagen
pJQ200mp18Km	Gene replacement plasmid, confers kan resistance and sucrose sensitivity by *sacB* gene	(41)
pJV7	pJQ200mp18Km containing *phaC* deletion allele in the multiple cloning site. *phaC* deletion allele has a *Swa*I restriction site inserted between 5′ upstream and 3′ downstream fragments of *phaC*	(40)
pCJB16	pET51b with *N*-terminal Strep2 tagged *phaC* gene containing a (G$_4$S)$_3$ linker between the tag and gene, confers amp resistance	This work
pCJB4	pJV7 with *N*-terminal Strep2 tagged *phaC* gene containing a (G$_4$S)$_3$ linker in the *Swa*I restriction site, gene replacement plasmid	This work
pCJB16-C319A	pCJB16 with C319A mutation, confers amp resistance	This work

Table 2

Primers used in this study

Name	Sequence[a]
phaCSTREPFW	5′-GAGTAGGGATCCCATGGGCGGCGGCGGCTCCGGCGGCGGCGGCTCCGGCGGCGGCTCCGGCGGCGGCGGCTCCGGCACCGGCAAAGGGCGGCGGCAGCTTCCAC - 3′
phaCSTREPRV	5′ - CTAGTGAAGCTTTCATGCCTTGGCTTTGACGTATCG CCC -3′
phaCC319A	5′ - ACGTGCTCGGCTTCGCGGTGGGCGGCACCA - 3′
phaCC319A-GC	5′ - TGGTGCCGCCCACCGCGAAGCCGAGCACGT - 3′

[a]Restriction sites underlined

Table 3

Activity Table for the Purification of Strep2-PhaC$_{Re4h}$.

Purification Step	Volume (mL)	Protein (mg)	Activity (U[a]/mg)	Total units	% Yield
Crude extract[c]	5.0	140	3.4	470	100
Soluble fraction	4.3	120	2.8	340	72
Insoluble fraction	2.1	15	8.7	130	28
Flow through	7.2	89	1.2	110	22
Washes	60	28	1.1	31	6
Pure sample	0.52	0.94	36	34	7

[a] One unit of enzyme activity is defined by one μmol of CoASH released per min.

[c] Crude extract for Strep2-PhaC$_{Re4h}$ purification originated from 1 g of cells.

Table 4

Molar ratios of Strep2-PhaC to PhaP1 to PHB in the HMW fraction of Strep2-PhaC$_{Re4h}$ compared to whole cells.

Purification step	Strep2-PhaC$_{Re}$	PhaP1	PHB
HMW fraction	1–3	4–9	1
Re2018 whole cells	0.1	0.6	1
Wt whole cells[a]	0.01	1	1

[a]Reference (25).